

promoting access to White Rose research papers



Universities of Leeds, Sheffield and York
<http://eprints.whiterose.ac.uk/>

This is an author produced version of a paper published in **Computers and Chemical Engineering**.

White Rose Research Online URL for this paper:
<http://eprints.whiterose.ac.uk/5433/>

Published paper

Caulkin, R., Ahmad, I., Fairweather, M., Jia, X. and Williams, R.A. (2009) *Digital predictions of complex cylinder packed columns*. *Computers and Chemical Engineering*, 33 (1). pp. 10-21.

<http://dx.doi.org/10.1016/j.compchemeng.2008.06.001>

DIGITAL PREDICTIONS OF COMPLEX CYLINDER PACKED COLUMNS

R. CAULKIN, A. AHMAD, M. FAIRWEATHER, X. JIA, R. A. WILLIAMS

Institute of Particle Science and Engineering,
School of Process, Environmental and Materials Engineering
University of Leeds, Leeds, LS2 9JT, UK

ABSTRACT

A digital computational approach has been developed to simulate realistic structures of packed beds. The underlying principle of the method is digitisation of the particles and packing space, enabling the generation of realistic structures. Previous publications (Caulkin et al., 2006, 2007) have demonstrated the ability of the code in predicting the packing of spheres. For cylindrical particles, however, the original, random walk-based code proved less effective at predicting bed structure. In response to this, the algorithm has been modified to make use of collisions to guide particle movement in a way which does not sacrifice the advantage of simulation speed. Results of both the original and modified code are presented, with bulk and local voidage values compared with data derived by experimental methods. The results demonstrate that collisions and their impact on packing structure cannot be disregarded if realistic packing structures are to be obtained.

Keywords: Packed beds, Digital packing algorithm, Cylindrical pellets, Voidage

1. INTRODUCTION

Many chemical and process engineering applications require the controlled packing of particulate solids, with packed column systems in particular employed in a wide range of disciplines, including applications of fixed bed catalytic reactors, filters and multi-tubular beds exchanging heat with an external medium. In industrial practice, the majority of these practical particulate bed systems consist of non-spherical particles that can be homogeneous or vary infinitely in shape and size. In addition, a typical matrix bed can be created under a variety of conditions, where the nature of the packing is governed by the particle and container size and shape, the loading method and intensity, and the subsequent treatment of the bed, resulting in either loose or dense packing. The final stable geometrical structure of a packed bed is therefore of utmost interest since it greatly influences the subsequent performance of a reactor. Despite this complex problem, many technical fields still make use of randomly packed beds of spheres for design and development purposes.

Macroscopic parameters such as packing density or voidage distribution are widely used to define bed structure in the design of such equipment. For mono-disperse packed beds, with tube-to-particle diameter aspect ratios (d_t/d_p) > 9 , the bulk voidage value is frequently assumed to be 0.40 for spherical particles and 0.30 for beds packed with equilateral cylinders (Vatani, 1996). Uniform, or plug flow distribution is also commonly assumed in these packed beds. However, while this may be a reasonable assumption at the centre of a large packed structure, it is not the case in the vicinity of the container walls or in low aspect ratio columns. In these situations the bulk voidage parameter does not provide sufficient levels of detailed information about the local structural properties of a bed, where considerable flow maldistribution can occur since large void spaces, and hence flow channels, exist. In the design and analysis of equipment where wall effects are significant, local porosity distribution, in both the radial and axial directions, is often utilised to provide a more detailed insight into packing structure. Past studies investigating the local characteristics of sphere and cylinder

packed beds include using experimental methods (Ridgway and Tarbuck, 1968; Gotoh et al., 1978; Lerou and Froment, 1986; McGreavy et al., 1986; Zou and Yu, 1996; Ismail et al., 2002; Di Felice and Gibilaro, 2004), analytical means (Moallemi, 1989; Papageorgiou and Froment, 1995; Afandizadeh, 1996; Wang et al., 2001) and empirical correlations (Martin, 1978; Cohen and Metzner, 1981; Dixon, 1988; Kubie, 1988; Mueller, 1992; Foumeny et al., 1993). Additionally, information on the packing of more complex pellet shapes (e.g. berl and intalox saddles, pall rings, hollow cylinders, grooved cylinders, etc...) and complicated container geometry is scarce.

As flow distribution through a bed is directly linked to its internal structure, the development of a fast, accurate and reliable method by which to predict the packing geometry of these often complex assemblages has the potential to bring about a step change to the current approach to new product design and optimisation of packed column reactors, which to date, has been based primarily on both physical tests, including utilising advances in scanning technology (both X-ray tomography and nuclear magnetic resonance imaging techniques (Kutsovsky, 1996; Seidler et al., 2000; Sharma et al., 2001; Richard et al., 2003; Aste et al., 2004; Zhang et al., 2006) have been proposed for this purpose), and empirical correlations, which are largely limited due to the restricted nature of the experimental data used in their derivation. This potential for change is particularly relevant as in recent years modelling techniques using computational fluid dynamic calculations (Logtenberg et al., 1999; Jiang et al., 2000, 2001; Maier et al., 2000; Krischke 2001; Zeiser et al., 2001; Einfeld and Schnitzlein, 2005; Sullivan et al., 2005; Dixon et al., 2006; Hlushkou et al., 2007) have progressed to the stage that they now have the ability to become a valuable tool in the field of research and design for many scientific and engineering disciplines, including catalyst packed columns. One of the main obstacles, however, is the necessity for an effective method of determining the three-dimensional geometric structure of beds packed with realistic shaped particles. With continued advances in computational power, the use of advanced numerical simulation techniques shows great promise (Nolan and Kavanagh, 1995; Dickinson and Knopf, 1998;

Nandakumar et al., 1999; Taylor et al., 2000; Abreu et al., 2003; Freund et al., 2003). Of the recent models proposed in the literature, many can predict the structure of sphere packed beds with reasonable accuracy. Several can also handle non-spherical objects, albeit at drastically reduced speeds compared to spheres. Significantly, however, many of these are unsuccessful in the prediction of accurate macroscopic properties when compared with experimentally measured beds of corresponding geometry.

In this paper, a digital-based approach to predicting the structure of non-spherical packed beds is described, which through the introduction of basic collision forces, semi-quantitatively predicts experimental bulk and local porosity values of various cylinder and ring packed columns. Particle packing is described using a digital approach (Jia and Williams, 2001) that avoids many of the difficulties suffered by conventional, vector-based packing models. The key step is the digitisation of both particle shapes and the packing space, with this method capable of handling particles of any shape and size in containers of any geometry. It is also capable of simulating physical phenomena such as the influence of vibration as well as the effect of collisions and the resulting particle interactions. In this work we describe the models and simulation conditions used and present the simulation results of numerous beds of varying complexity, using comparisons with experimental results as the basis for model validation. Reported results are packed with cylindrical/ring pellets, with the data divided into two main sections; i) mono-sized equilateral cylindrical pellets containing holes (of different sizes) through the centre of the particles, which are packed in conventional containers (Table 1) and; ii) solid cylindrical pellets packed into shell-side containers (Table 2). In shell-side packed beds the particles reside on the outer side of either single or multiple tubes contained within a 'shell'. This type of packed bed arrangement is widely used in fixed bed catalytic reactors, with the catalyst particles on the shell-side and the heating or cooling medium flowing inside the tubes. There are usually a number of these tubes arranged inside the reactor in such a way that they form equilateral triangular arrays.

2. PACKING MODELS AND EXPERIMENTAL WORK

2.1 The DigiPac and DigiCGP Models

To handle particles other than the simplest shapes, conventional vector-based packing algorithms commonly use either sphere-composites (Nolan and Kavanagh, 1995) or surface meshes (Dickinson and Knopf, 1998) to approximate individual particle structures. In principle, arbitrary shapes can be approximated by either of the two methods for use in particle simulations. In practice, however, computational difficulties severely restrict their application. For example, coding arbitrary shapes in a computationally cost efficient manner by using as few primitives as possible for the sake of speed, while meeting the minimum requirements in accuracy, is a painstaking process and is difficult to automate. Dealing with collision and overlap detection is another major computational hurdle as developing and implementing an efficient and robust algorithm to detect collisions and overlaps between complex shapes is often the most time-consuming part of a simulation.

Images on a computer screen are all pixel based. This ‘pixelation’ (2D) or ‘voxelation’ (3D) of objects and of the packing space is the basis of the code called DigiPac. In this algorithm, digitisation is utilised for representing and packing objects regardless of structural complexity. Therefore any arbitrary shape is represented in three-dimensions as a coherent collection of voxels and the simulation volume as well as the container into which the particles are packed is converted into a three-dimensional lattice grid. Simple analytical shapes, for which library support is provided by software development tools (e.g. Visual C++) are created and digitised directly in the computer memory. More complex shapes, for example real particles, taken either from photographic or scanning electron microscope (SEM) images, or as volumetric outputs from commercially available 3D scanners (e.g. X-ray microtomography), can be used directly by the digital algorithm. This approach is easily amendable to modern (digital) means by which the raw shape information is obtained and stored in the first place. Since the packing space and container are digitised also, using a

container with a complex boundary and internal geometry presents no additional difficulties or drawbacks for the model.

In a simulation using this code, the particles are allowed to move randomly, one grid at a time, on a square lattice. In three dimensions there are 26 possible directions, six orthogonal and 20 diagonal. It is convenient to treat diagonal moves as composed of two orthogonal moves. For example, a move in the lower-left direction can be thought of as a downward move followed by a left move. In order to encourage particles to settle, the upward component of a move is only accepted with a so-called *rebounding probability*. This results in a directional and diffusive motion for the particles, similar to a random walk-based sedimentation model. This diffusive movement helps the particles to effectively penetrate and explore every available packing space. This movement of particles over a grid makes collision detection much easier as it can be checked whether two particles occupy the same grid space at the same time. This significantly reduces computational time compared to other algorithms where overlap detection is mostly by mathematical comparisons. Since particles move only one grid at a time, the overlap detection procedure ensures that one particle will not jump over, or enter the hollow part, of another particle during packing. It also allows solid particles to be represented by their outlines, which substantially speeds up the simulation process since fewer voxels per particle need to be processed for each trial move. The ease of overlap detection significantly increases the computational efficiency and drastically reduces the coding effort in software implementation. In addition, unlike conventional methods, at a given resolution the computing resources (i.e. memory and CPU time) required for the simulations do not increase with the complexity of shapes, and as computations using the digital code are performed mainly on integers used to store locations of voxels, it runs as fast on general purpose PCs as on the more expensive workstations.

Although the original version of the DigiPac algorithm does not explicitly involve physical forces, some effects of physical interactions can still be simulated. Since particles are allowed

to move sideways as well as up-down, even after they form part of the packing, the effects of high frequency, small amplitude vibrations can be simulated. The vertical vibration is controllable, by means of the rebounding probability, a user-defined model parameter. In a simulation of particle packing under the influence of gravity, the preferential direction is downward. A value of zero means that particles are never allowed to move upwards so they settle down as quickly as possible. A value of one means that particles have an equal probability to move up or down, therefore they remain suspended until more particles are added from the top, resulting in higher particle concentration and more collisions at the top, thereby forcing the particles to diffuse downwards. For particles already packed in the bed, a non-zero rebounding probability provides a non-physical way to simulate the effects of vibration where particles, particularly those on the top surface of the packed bed, jump up and are allowed extra time and space to find a more fitting position in which to settle. For this reason, for a given mixture of particles, a higher rebounding probability tends to result in a denser packing structure. Typically, a value between 0.2 and 0.5 is used in calculations.

In this work, two versions of the DigiPac model are investigated for the packing of non-spherical objects. The original version of the code is completely probabilistic in nature and uses random walks to simulate particle movement. In the modified version particles are still represented digitally, so the computational advantages of ease and speed of collision and overlap detection are retained. While this version is also stochastic, the difference is it makes use of collisions to guide particle movements (Collision Guided Packing or DigiCGP). To simulate individual collision forces that act on every particle would come at a high computational cost. For beds that consist of relatively large and more or less identical pellets, and for trend finding exercises, a quicker, albeit less accurate, solution is more desirable. The DigiCGP code is designed for this purpose. It is a half-way house solution, between the two extremes of completely probabilistic and wholly deterministic. In the version used herein, collision points are identified in the lattice grid and each pair of colliding voxels is then assigned a nominal impact force of one. For torque calculation the direction of the nominal

impact force is taken to be normal to the contact face of the colliding pair of voxels. The net torque vector is subsequently used as the axis of particle rotation in the following step. The angle of rotation is still random, but is capped to give a maximum swept distance of no more than a few pixels during the rotation. To calculate the net force, the direction of an impact force is taken to be along the line joining the collision point and the centre of gravity of each particle. The reason for this can be illustrated by an example where a sphere is dropped on an inclined surface. Due to digitisation, at the pixel level, both sphere and slope surfaces are staircases. If the nominal impact forces were assumed to be normal to the local contact faces, in the absence of any contact resulting in horizontal force, the sphere would simply bounce vertically on the staircase rather than travel down the slope. Therefore a change in the direction of impact force is a simple and effective short-cut to ensure this is avoided. For translational movement the net collision force is normalised against the largest component, so each force component is now between 0 and 1. This is then used as the probability of moving the particle by at most one grid cell at a time along each principal axis in the lattice grid, as in the original code. Thus, instead of completely random movement, the directions of particle movement and rotation are now guided by collisions. It should be noted that the above treatment does not include voxel-level friction or any other forces tangential to a contact. Particle-level friction is partially accounted for by the roughness of the digital surfaces. The method also neglects inertia effects as particle velocity is neither calculated nor stored. All these omissions are for the sake of computational speed and result in a simulation time comparable to that of the original DigiPac code. For dense systems involving large and identical objects, such as the packed columns under investigation here, the simplification is justifiable and acceptable, as it results in semi-quantitative predictions as demonstrated later.

2.2 Experimental Methods

The experimental investigations of packed columns reported in this paper were obtained both from the literature (Roshani, 1990) and also by the co-authors using similar data collection methods. Cylindrical containers were constructed by boring into solid PVC rod at the required

internal diameters. The height of all the containers was 100mm despite the pellets only being packed to approximately 60% of this height. The additional height was to enable the lathe to grip the container securely. Where applicable, the internal tubes running axially through the beds were fixed in place by adhesion to the container base in the required configurations, and were constructed from the same material. Lead ballast was used as the packing material, which was chosen partly for its softness, so to avoid blunting the machine tool when increments of the bed were shaved off by the lathe, and also because lead can be polished to obtain a strong contrast between the particles and resin which improves the reliability of the data derived from digital images. To ensure good adhesion between the pellets and the resin, the outer coating of the particles was removed prior to packing by gentle rotation in a container of sand, thus increasing the surface roughness of the particles and enabling a stronger bond to be formed. For bonding purposes, Ampreg 20 resin was utilised which is a modern generation laminating resin. The resin combines good mechanical properties, low viscosity and generous working times, which make it ideal for this application. The resin mixture was dyed by addition of Oxford Blue prior to use in order to increase the contrast between the lead particles and the resin.

The pellets were introduced into the container in small batches (approximately 10 at a time), followed by gentle tapping after each addition to allow for the exploration of available packing spaces. When each layer, one particle thick, was formed, a small amount of resin mixture was poured slowly and uniformly over the particles, taking care to fill any gaps and ensure that no air pockets remained. The next layer of particles was then introduced into the bed via the same procedure. This method was repeated until the container was packed to a height of approximately 60mm and aimed to simulate a poured randomly packed bed. After solidification each packed bed was periodically turned in a lathe and axially 'sliced' to expose 50 consecutive cross-sections, shaving off 1mm each time. The accuracy of the lathe means that axial cuts were performed to within ± 0.001 mm. Each time, the newly exposed cross-section was wetted and polished using silicon carbide paper (P1800 grade) to improve

contrast between the pellets and resin mixture. A digital snapshot of each slice was then captured and saved so that each image could be retrieved later for subsequent analysis using the colour contrast method. A packing height of 60mm was deemed ample for the required number cuts to the bed. The accuracy of all bed dimensions is $\pm 0.05\text{mm}$. By magnifying the images of the test sample cross-sections to the maximum capacity of the VDU screen employed, the highest possible resolution was achieved (8bit image of 512x512 pixels).

To calculate the local voidage of the bed, defined as the ratio of the void volume in an element of bed volume (i.e. the free paths available in a specific section of bed volume), the area of interest was delineated first with rectangular and then with circular measurement frames, which facilitated further analysis of the specified area. The software used then converted the images to a binary form. Once calibrated, 50 consecutive annular rings were applied by the software which corresponded to the pre-calibrated area of the image. The number of black and white pixels in each annulus was then counted and this ratio yields the local voidage in each given annulus. Radial voidage profiles were calculated by axially averaging the local area voidage of consecutive annular rings of the corresponding sections over the whole height of the bed. This approach thus facilitates the study of a three-dimensional history of the void fraction, both axially and radially. This technique has great advantages, among them being the ability to retrieve and analyse stored images, and the unique quality of the data obtained. Each measured bed was packed a minimum of four times (see Tables 1 and 2) with the above process repeated for each bed, as were each of the predicted beds (four trial runs per bed type). The corresponding results of each trial were then averaged to give a single experimental and simulation result for each bed, which could then be compared like-for-like. This process was undertaken for each of the packings reported in this paper.

2.3 Data Extraction

For digital packing structures, voidage distribution is easily calculated by counting the number of solid voxels and dividing the count by the total number of grid cells within the corresponding packing space. This procedure applies to both simulated and optically analysed experimental packing structures once converted to digital format. Firstly we consider the voidage in the axial direction (i.e. from the base of the bed upwards towards the bed inlet). The porosity of each of the 50 bed slices (experimental slice = 1mm thickness; simulation slice = 5 pixels thickness at a resolution of 0.2mm/voxel) is calculated automatically within both the algorithm and the software package used for experimental data analysis by calculating the ratio of solid to empty voxel sites. These data points are then plotted against axial distance from the base of the container in particle diameters. To calculate radial voidage, the packed column is divided into equally spaced concentric rings. Again, voxel counting is used, this time for each ring over the total height of the bed, rather than each slice as performed for axial voidage. The resulting values are then plotted against radial distance in particle diameters from the retaining wall. Bulk voidage measurement is determined for the beds reported in this paper by averaging the axial voidage of resulting beds with end effects excluded. A more detailed explanation of the procedure used for data extraction of one simulated bed is provided in the appendix.

3. RESULTS AND ANALYSIS

The majority of existing research on packed beds is centred on the packing density/voidage profiles of sphere packed structures. In relatively recent years, research on beds of cylindrical packings and reactors with embedded tubes has increased (Schneider et al., 1990; Li et al., 1991; Nolan and Kavanagh, 1995; Zou and Yu, 1996; Dixon et al., 2006; Zhang et al., 2006). A number of these cylindrical (and occasionally rectangular) packed beds are simplified versions of those used in industry which contain pellets of simple geometric description. Hence, little information exists about how bed structure is affected in such types of packed columns. It is therefore pertinent to establish a basic understanding of the structure of such

beds and to ascertain the accuracy with which the DigiPac code (original and modified) can predict the subsequent bulk and local porosities. In view of this, numerous beds derived using the described models and packed with cylindrical and ring shaped pellets, and different configurations of internal tubes, are examined in terms of structure by numerical analysis for direct comparison with beds created by experimental means.

As the final bed structure relies upon the packing history, whereby different packing conditions can result in different structural arrangement, the packing models allow a range of options to be considered that control how objects are introduced and how they behave once added. Specific variables were selected to mimic the packing conditions of the experiments. This included adding relatively few randomly orientated particles each time over the whole area of the container, which were permitted to free-fall and change their orientation upon contact with other particles or the container walls/base. In the experiments, the pellets were then allowed to reach a stable, stationary position following gentle tapping with a ruler to the sides of the container, before following particles were added from above. This allowed each layer of pellets ample opportunity to explore and pack closely with its neighbours before resin and subsequent layers of particles were introduced, 'locking' the lower pellets into place, thus preventing these particles from further rearrangement. The model recreated this gentle tapping, or vibration, by utilising a rebounding probability of 0.4. The specific variables used to obtain data for one sample result are provided in the appendix.

For clarity, the results reported here are divided into two sub-sections. The first section (3.1) presents hollow cylinders (HC) packed into conventional containers. They are comprised of five pellet arrangements, with each type individually packed in a single container, as given in Table 1. The second section (3.2) shows a total of three sizes of solid cylindrical pellets packed into three configurations of shell side beds as detailed in Table 2. Multiple trials of simulated beds were packed and analysed for each bed type and at least as many corresponding experimental runs were performed for each example. The bulk porosity, the

most common packed bed parameter that is used to compare numerical simulations with experimental/analytical data is also presented in Tables 1 and 2. The mean bulk voidage was obtained by averaging the axial voidage profiles of the replicate beds in the middle section of the packed columns. Standard deviations were also calculated from the axial voidage profiles and are a measure of porosity variations within the packed beds, not between the beds. These values are therefore an indicator of how uniform the bed structures are in the bulk section in each case. Also, next to each averaged bulk DigiCGP simulation value is the percent error as compared with the experimental data. The modified packing algorithm, using this dimensionless packing parameter provides good results with percent errors less than 5% for bulk voidage. The packed bed parameters of radial and axial porosities are also used to compare the simulation accuracy of the algorithm to the experimental data, and results are presented in Figures 2 to 5. The average CPU time taken to complete a single simulation (with multiple random particle rotation) was typically less than one hour using a desktop PC with a Pentium 4, 2GHz CPU and 512Mb RAM. Significant speedup was achieved as the simulations were run on a multi-CPU shared memory computer, with multi-thread software implementation.

Figure 1

3.1 Hollow Cylinders (HC) in Conventional Beds

The beds considered in this section are packed with single-size equilateral cylinders (d_p , $h_p = 12.7\text{mm}$). The cylindrical container size is also kept constant for the beds investigated ($d_t = 103\text{mm}$). The only variable between each of the five beds is that of the internal structure of the packing material. As seen from Figure 1a and Table 1, the particles (labeled as HC1-5) range from solid cylindrical pellets to cylinders containing various sized and numbered internal holes running axially all the way through the pellets. These represent generic catalyst particles, with internal holes to increase reactive surface area.

Table 1

The Digi-code simulated beds were configured to utilise the same set-up conditions as the experiments undertaken by Roshani (1990). This included allowing the pellets to rotate randomly during free-fall into the container and in their subsequent rearrangement once they formed part of the packing structure by means of selecting a rebounding probability of 0.4, which reflects the treatment of the experimental beds in between the filling of individual layers of pellets. Each of the measured beds investigated by Roshani (1990) was packed a total of five times, and in each instance the local voidage was measured and recorded. The voidage values presented are therefore an average of the five trial runs in order to produce a single representative plot for each type of bed. For the predicted results, four simulation runs for each version of code were undertaken and averaged for each bed type. The three resulting averaged plots for each bed, one measured and two predicted (DigiPac and DigiCGP) were then compared directly. Five trial runs per bed type were chosen as a suitable average by Roshani (1990) in order to gain representative results. The lower value of four trials per bed was used by the authors when investigating the two prediction models as it was determined that undertaking additional trials did not provide any noticeable change in the algorithm results in terms of the reproducibility of the average voidage values.

Figure 2

Figure 2 compares the measured and predicted results for HC pellets packed into conventional cylindrical columns. Radial voidage is presented down the left-hand column and axial voidage along the right-hand side column. The distance is scaled by pellet diameters from the retaining wall and base, respectively. Beginning at the container wall and moving towards the bed centre for all five configurations, the radial voidage distribution varies in an oscillatory manner with the amplitude of local voidage oscillation becoming progressively damped with distance from the wall, although remnants of it remain in existence throughout all the beds

due to the limited d_t/d_{pe} ratio which prevents the formation of a core zone. Each of the beds (HC1-5 predicted and measured) have a radial voidage value of 1.0 at the container wall which decreases to a minimum value at around $0.5-0.75d_p$ before rising to a peak at approximately $1.0d_p$. This is predicted qualitatively by both the DigiPac and DigiCGP models for all five bed types. However, observing more closely the radial voidage of the predicted beds in this near wall region (0 to $1.0d_p$), it is seen that moving from bed HC1 to HC5 the DigiPac predicted radial voidage becomes increasingly less accurate where larger particle hole sizes are employed in the respective beds, which generally leads to increased disruption in porosity, particularly in the near-wall region. The modified CGP code however is somewhat more successful, predicting the voidage of each bed semi-quantitatively.

In bed HC1, where the packing material consists of solid cylinders the measured radial voidage within one equivalent particle diameter of the wall takes the form of a smooth, uninterrupted upward curve. This is qualitatively reproduced by the DigiPac model and more accurately by the DigiCGP code, as is the remainder of the bed whereby the location of the maxima and minima predicted voidage largely correspond with those of the measured data. For bed HC2 in which the particles contain a single small hole (2mm) the measured radial voidage between the outer wall and first equivalent particle diameter takes the form of a largely smooth curve with the exception of a slight disruption in voidage at $0.5d_p$. Although the version of the original code completely fails to predict this, it is qualitatively reproduced by the DigiCGP algorithm. Beds HC3 and HC4 continue the trend where the measured radial voidage displays increasing disruption, in the form of an increasingly broken curve, within one particle diameter of the outer bed wall which in part is caused by the progressively increasing hole size (and so higher internal voidage) of the pellets. As seen in bed HC2, the original code fails to predict this interruption to the voidage curve at $0.5d_p$ for the particles containing central holes measuring 4mm and 6mm respectively, only becoming inline with measured data at the minimum voidage point around $1.0d_p$. However, the modified DigiCGP version of the code semi-quantitatively and qualitatively predicts the measured data. The final

bed in this section, HC5, which contains four 2mm holes arranged in a quadrant, displays less significant disruption in radial voidage close to the wall than the previous bed, HC4. The experimentally derived plot of radial voidage that results from particles of this type is visually very similar to that displayed by the particles containing a single 4mm (medium) sized hole (the pellets in beds HC3 and HC5 have identical d_p and d_t/d_{pe} values), although the overall voidage is noticeably elevated when compared to that of bed HC3. This is most likely due to the four individual holes of pellet type HC5 being spread over a wider area of the ends of the pellet. It is seen again that the DigiPac algorithm fails to reproduce this voidage structure close to the wall, and even the modified CGP version fails to predict a truly qualitative match. However, after $1.0d_p$ the DigiCGP predicted radial voidage average can be described as qualitatively matching that of the measured bed.

Many of the same trends and characteristics observed for radial voidage are also seen when examining the axial voidage profiles of the same beds, whereby DigiPac qualitatively and DigiCGP semi-quantitatively predicts the voidage from the base of the beds upwards. It should also be noted that the beds packed with hollow cylinders were packed to a relatively low height of approximately four particle diameters. The main reason for this is that we are more interested in local voidage in the radial direction rather than axial, as radial analysis shows greater variation between different packing materials. Axial voidage is still important, but tends to fluctuate around a well defined mean, so tells us less about the individual packing structure of a particular bed. Also, end effects tend to dissipate sooner than wall effects due to the flat container base as compared to the curved side wall of the container. Therefore, only a relatively short packing height was used, as end effects became insignificant beyond approximately three particle diameters. However, for the packed structures containing internal tubes (Section 3.2), an increased packing height was used (typically between 6-10 particle diameters) due to the greater amount of voidage fluctuation, and hence extended end effects, in the axial direction caused by the presence of these tubes.

3.2 Solid Cylinders in Shell-Side Packed Beds

The data presented in this section is the result of solid cylindrical pellets packed into shell-side containers. The dimensions of the experimental beds investigated by the authors were determined by scaling down the dimensions of industrial packed columns. In some of these beds, it is common that there is a separation distance between the centres of any two tubes as low as 64mm (Ahmad, 2000), with the diameter of the internal tubes measuring 50% of this distance. To simulate these dimensions in both experimental and simulation format, the packed beds were scaled down by a factor of four. Therefore, the distance between the centres of any two internal pipes was 16mm, with the outer diameters of these internal tubes measuring 8mm. A relatively large container diameter, d_t , is used for all beds in order to ensure that the retaining bed wall is a sufficient distance from the internal pipe(s) so as not to have any appreciable effect on porosity around the internal tube(s). The dimensions of the shell-side beds investigated in this paper are detailed in Table 2.

Table 2

Figure 3

Figure 3 shows local voidage plotted against distance from the outer wall (in particle diameters) for beds CA3 and CA4. That of the first bed, bed CA3, shows that from the outer wall radial voidage initially decreases in amplitude from 1.0 to a minimum of 0.11, then proceeds as a damped oscillatory wave until the central tube is approached. At this point, $6.5d_p$ from the outer wall, the decreasing cyclic variation ends and the voidage rises sharply to 1.0. The second CA bed investigated exhibits similar characteristics to bed CA3, with the single difference between the two beds being that CA3 is packed with equilateral cylinders whereas bed CA4 is packed with non-equilateral cylinders, and so the difference in particle height can be attributed to the differences seen in radial and axial voidage between the two beds.

When cylindrical particles are introduced into a packed bed, the container wall exerts some influence on the orientation of the outermost cylinders forcing a row of pellets to be formed along the outer wall. The second row of cylinders then rest in the cusps formed by the packings in the first row. Therefore, moving inwards from the wall to the bed centre, the trend is repeated, with each subsequent row more random than the previous. Due to the near identical footprint of equilateral cylinders (in terms of area) regardless of whether a pellet sits on its end or lies on its side, the rows remain more ordered than if packed with non-equilateral cylinders. This goes some way to explaining why the equilateral cylinders in bed CA3 display a greater degree of local voidage oscillation than the non-equilateral particles in bed CA4. The radial voidage of the CA beds (as illustrated in Figure 1b) predicted by the respective DigiPac and DigiCGP codes qualitatively and semi-quantitatively agree with the experimental data. Analysing the radial voidage of beds CA3 and CA4, it is seen that the lowest values attained near the outer wall are, for bed CA3 0.11 measured (0.15 DigiPac and DigiCGP predicted), and for bed CA4, 0.20 (0.18 and 0.22, respectively). The wall effect is more pronounced at the outer bed wall than at the internal tube wall located in the centre of the bed. This is demonstrated by the amplitude and extent of the sinusoidal waves in these beds, where near the outer wall the wave amplitude of the voidage profile is greater and extends further into the packing than it does near the internal tube for both beds. The reason for this greater expanse of voidage in this area is because the outer wall has a larger circumference than that of the centre tube, therefore there is a greater area at the outer bed wall for particles to make point contact with compared to the centre tube wall, and hence voidage at the outer wall will be enhanced due to the greater cumulative disruption. From the axial voidage plots of the two CA beds it is apparent that the equilateral cylinders of bed CA3 cause additional disruption in terms of end effects than is seen in bed CA4. In bed CA3, the oscillatory wave of voidage variation extends approximately $5.5d_p$ into the packed structure. However, for DigiCGP predicted voidage it only persists for $3.5d_p$ and for the original DigiPac code it is even less. Experimentally, bed CA4 displays end effects for $2.0d_p$ into the bed, with predicted results also extending for this length from the base of the column. A possible explanation for this is

due to the differences in cylinder height making up the two beds. The non-equilateral pellets in bed CA4 have the same diameter as the equilateral cylinders of bed CA3 but are significantly shorter, meaning the equivalent particle diameter of these pellets is significantly less, so the voidage disruption caused by these particles at the base of the bed is able to dissipate sooner and hence does not extend as far into the packing structure.

Figure 4

Figure 4 presents the comparative measured and predicted local voidage of beds TA1 and TA2, containing equilateral cylinders with particle diameters measuring 8.6mm and 5.3mm, respectively. Analysing the radial voidage for bed TA1 it is seen that voidage decreases from 1.0 at the outer wall to a minimum of 0.19 (0.33 DigiPac; 0.23 DigiCGP) at $d_p = 0.75$. The radial voidage then proceeds as a damped oscillatory wave until the central structure of the three internal pipes is approached. Here, at approximately $2.75-3.0d_p$, the waveform ends and the voidage rises to a peak of 0.64 for the experimentally measured results and 0.60 for the voidage predicted by DigiCGP (0.53 DigiPac). After $4.0d_p$, the voidage resumes as an oscillatory wave until the bed centre is reached. Bed TA2, which is packed using smaller equilateral cylinders than bed TA1 reveals many of the same features and characteristics. The main difference for bed TA2 is that the radial voidage extends for a greater number of equivalent particle diameters, due to the smaller particles that are packed into a container of identical size to that of bed TA1. Therefore, the opportunity exists for a greater number of smaller particles to fit into a space which is the same size as that used to pack larger particles. The minimum porosity recorded for bed TA2 again occurs at $0.75d_p$ from the container wall, as in bed TA1, with a measured value of 0.18 (0.22 DigiCGP). At its peak radial voidage around the three internal tubes, bed TA2 has a maximum value 0.57 (0.56 CGP). For radial voidage, the predicted voidage in particular displays a greater span of elevated porosity in the vicinity of the three internal tubes. The likely reason for this is that because the cylindrical particles in bed TA2 are smaller than those of bed TA1, it would be possible for a larger

number of these pellets to occupy the space between the tubes in bed TA2. This creates a greater number of boundaries between particles, which in turn leads to an extended area of elevated voidage. Figure 4 illustrates that for this triangular shell-side bed arrangement at least, smaller cylindrical particles result in an overall lower radial voidage. This demonstrates that smaller particles, as with spheres (Caulkin et al., 2007), form a more compact packing within shell-side beds than larger particles.

The TA beds investigated in this paper do not provide information on how each internal tube individually affects the voidage in the bed, due to influences of the neighbouring pipes affecting how the particles are arranged. As a result of this, two further beds containing only one tube each, but otherwise identical to the TA beds, were investigated for local voidage. From Figure 1(c, d) and Table 2, it is seen that the corresponding beds (TA1 and OA1; and TA2 and OA2) contain the same size particles and same container diameter.

Figure 5

The OA beds in Figure 5 contain only one internal tube, located in the same position as one of the tubes in the TA beds. This is to allow a direct comparison between the OA and TA beds, permit the effects of multiple tubes on local voidage to be assessed, and also investigate the ability of the algorithm in predicting such changes. The similarities that are seen to exist between the two bed types, in not only the measured beds but also the DigiPac and DigiCGP predicted beds, extend throughout the entire bed for each particle size investigated. The radial voidage of bed OA1 once again takes the form of a damped oscillatory wave that proceeds until the single internal tube is approached. At this point, around $3.5d_p$, just as in bed TA1, the voidage increases slightly to a measured peak of 0.55 (0.53 CGP) before continuing in a damped manner. Bed OA2 also displays similar characteristics to bed OA1 and TA2, with an extended elevated value between $4.0d_p$ and $5.3d_p$, peaking at a value of 0.43 (0.40). The location at which the peak value occurs again corresponds with that of bed TA2. It is

observed from the beds investigated that the DigiCGP model predicts, in a semi-quantitative manner, and within accepted error margins, the bulk and local voidage of the experimentally investigated beds.

4. DISCUSSION AND CONCLUSIONS

Rather than predicting the structure of sphere packed beds which have been widely studied by previous researchers (partly due to the simplicity of such beds and partly because spheres require less CPU time and memory to simulate than more complex particles) this work has considered prediction of the structure of cylinder packed beds which are widely accepted as more challenging to simulate due to the complex manner in which the particles may orientate. These types of beds were investigated in an attempt to validate the modified DigiCGP code against experimentally derived structures, and to show that it has the ability to reproduce the bed structures of more realistic scenarios that are found in industry, i.e. during the charging of catalyst pellets in beds containing internal pipes. In the design of such beds, empirical correlations derived from sphere packed beds are often utilised, with the addition of correction factors in order to estimate the structure of a given bed.

The conclusions that can be drawn from the comparative results for the HC beds are that hole size, and therefore overall particle volume, contribute to the degree of disruption to the ideal smooth local voidage profile of solid cylinders. Larger hole size and higher internal porosity of a group of identical pellets leads to more disruptive local voidage, which manifests as a less smooth curve, particularly near the outer bed wall ($< 1.0d_p$). This conclusion is supported by results for pellet type HC5 which has an equal equivalent particle diameter ratio to pellet group HC3. Bed HC5 displays a similar, albeit elevated, voidage profile to the bed containing pellets with 4mm diameter holes. Therefore, the configuration of the holes appears to be of secondary importance to the overall internal particle voidage in terms of the local voidage profile. Where the configuration of internal holes does take precedence is in the bulk voidage

of the beds (see Table 1), where bulk voidage increases in-line with particle hole size, but also with the configuration and area these holes cover, which accounts for the elevated local voidage of bed HC5 in comparison with the other four HC beds. This experimentally observed trend is reproduced by DigiCGP with good accuracy, whereby precise force calculation is not important. What is important is that upon collision, objects have the tendency to move and rotate apart rather than following a random trajectory, as is the case with the original version of the model. For voidage analysis of cylinder and ring packed beds, this approach is shown to produce reasonable results (error typically < 5%), with good degrees of reproducibility, which make it ideal for trend finding exercises. However, for analysis of other variables, such as pellet orientation distribution, preliminary tests suggest that this simplified method leads to results that are not always accurate. Therefore, for cases where such criteria are important, a more deterministic approach would be required.

It has also been found that the original DigiPac code has difficulty accurately predicting the voidage close to the retaining wall structure. From Figure 2 it appears that when no internal voidage is present within the particles (bed HC1), DigiPac predicts the local voidage of a bed with reasonable accuracy. However, the HC1 particles are equilateral cylinders, meaning that on a global and local scale, a particle will appear similar regardless of whether it is upright or oriented on its side. When the same sized particle contains a distinctive internal structure, however, the voidage of that particle will appear different depending on the orientation in which it settles. Beyond $1.0d_p$ from the wall, DigiPac qualitatively predicts radial voidage for the majority of particle types investigated. A possible reason why DigiPac fails to predict the pattern of voidage close to the retaining walls is because it is primarily a geometric packing model, so does not consider particle interaction forces. With spheres, this is rarely a problem as particle orientation does not have any effect upon local voidage values. With cylinders however, this lack of any consideration of actual interaction forces, particularly in the near wall region where there would be interaction of particles with the container wall in addition to other pellets, fails to reproduce the experimental bed structure.

Comparing the TA beds with the OA beds reveals that TA1 and TA2 consistently have higher radial voidage than beds OA1 and OA2, respectively. The only difference in these two bed types is the number of internal tubes. In the TA beds, there are three tubes that give rise to three overlapping wall effects within the bed. Hence, an elevated voidage profile is seen when compared with the OA beds that contain only a single tube. Comparing bed TA1 with TA2, and bed OA1 with OA2, a lower radial voidage results for the second bed group as TA2 and OA2 are packed with smaller cylinders which form more compact packing throughout the beds. In Figure 5, the rise in radial voidage for the OA beds, after the profile has taken the form of a damped oscillatory wave (i.e. as the tubes are neared) is not as great as in Figure 4 for the TA beds. As only one tube is present, opposed to three in the TA beds, the distortion from the true radial voidage is less for the OA beds.

In this paper an improved and reliable predictive method has been shown to be capable of predicting the bulk and local voidage of beds of complex geometry with a reasonable degree of accuracy. The resulting bed structures have been demonstrated to agree well with experimental data which, combined with its user-friendliness and low running costs in terms of memory and CPU time, demonstrates the potential of the code for use in the design and development of such beds by means of coupling with other computational methods such as the lattice Boltzmann method. Development has also recently commenced to incorporate further particle interaction forces into the code in a Distinct Element Method, or DEM, fashion. Once this DigiDEM is developed and applied, still more accurate results, particularly in regions near the walls, can be expected as the code will then be deterministic in nature, with quantitative correlation with physical properties.

NOMENCLATURE

d_p	Particle diameter
h_p	Particle height
d_{pe}	Equivalent particle diameter
d_t	Cylindrical tube diameter (inner)
d_t/d_{pe}	Tube to-equivalent particle diameter ratio
h_t	Packed bed height
d_{te}	Equivalent tube diameter
d_{te}/d_{pe}	Equivalent tube-to-equivalent particle diameter ratio

REFERENCES

- Abreu, C.R.A., Tavares, F.W. and Castier, M. (2003). Influence of particle shape on the packing and on the segregation of spherocylinders via Monte Carlo simulations. *Powder Tech.*, **134**, 167-180.
- Afandizadeh, S. (1996). *Structural aspects of packed bed design using statistical methods*. PhD Thesis, University of Leeds.
- Ahmad, A. (2000). *Voidage variations in shell-side packed beds*. PhD Thesis, Dept. Chemical Engineering, University of Leeds.
- Aste, T., Saadatfar, M., Sakellariou, A. and Senden, T.J. (2004). Investigating the geometrical structure of disordered sphere packings. *Physica A*, **339**, 16-23.
- Caulkin, R., Fairweather, M., Jia, X., Gopinathan, N. and Williams, R.A. (2006). An investigation of packed columns using a digital packing algorithm. *Comp. & Chem. Eng.*, **30**, 1178-1188.
- Caulkin, R., Ahmad, A., Fairweather, M., Jia, X. and Williams, R.A. (2007). An investigation of sphere packed shell-side columns using a digital packing algorithm. *Comp. & Chem. Eng.*, **31**, 1715-1724.
- Cohen, Y. and Metzner, A.B. (1981). Wall effect in laminar flow of fluids through packed beds. *Jnl. Am. Inst. of Chem. Eng.*, **27**, 706-715.
- Dickinson, J.K. and Knopf, G.K. (1998). *Generating 3D packing arrangements for layered manufacturing*. Rensselaer's International Conference on Agile, Intelligent & Computer Integrated Manufacturing, Troy, New York.
- Di Felice, R. and Gibilaro, L.G. (2004). Wall effects for the pressure drop in fixed beds. *Chem. Eng. Sci.*, **59**, 3037-3040.
- Dixon, A.G. (1988). Correlations for wall and particle shape effects on fixed bed bulk voidage. *Can. Jnl. Chem. Eng.*, **66**, 705-708.
- Dixon, A. G., Nijemeisland, M. and Stitt, E. H. (2006). Packed tubular reactor modelling and catalyst design using computational fluid dynamics. *Adv. Chem. Eng.*, **31**, 307-315.
- Eisfeld, B. and Schnitzlein, K. (2005). A new pseudo-continuous model for the fluid flow in packed beds. *Chem. Eng. Sci.*, **60**, 4105-4117.
- Foumeny, E.A., Benyahia, F., Castro, J.A.A., Moallemi, H.A. and Roshani, S. (1993). Correlations of pressure drop in packed beds taking into account the effect of containing wall. *Chem. Eng. Sci.*, **36**, 536-540.
- Freund, H., Zeiser, T., Huber, F., Klemm, E., Brenner, G., Durst, F. and Emig, G. (2003). Numerical simulations of single phase reacting flows in randomly packed fixed-bed reactors and experimental validation. *Chem. Eng. Sci.*, **58**, 903-910.

Gotoh, K., Jodrey, W.S. and Troy, E.M. (1978). Variation in the local packing density near the wall of a randomly packed bed of equal spheres. *Powder Tech.*, **20**, 257-260.

Hlushkou, D., Khirevich, S., Apanasovich, V., Seidel-Morgenstern, A. and Tallarek, U. (2007). Pore-scale dispersion in electrokinetic flow through a random sphere packing. *Analy. Chem.*, **79**, 113-121.

Ismail, J.H., Fairweather, M. and Javed, K.H. (2002). Structural properties of beds packed with ternary mixtures of spherical particles: part II - local properties. *Trans. IChemE*, **80**, 645-653.

Jia, X. and Williams, R.A. (2001). A packing algorithm for particles of arbitrary shapes. *Powder Tech.*, **120**, 175-186.

Jiang, Y., Khadilkar, M. R., Al-Dahhan, M. H. and Dudukovic, M. P. (2000). Single phase flow modelling in packed beds: discrete cell approach revisited. *Chem. Eng. Sci.*, **55**, 1829-1844.

Jiang, Y., Khadilkar, M. R., Al-Dahhan, M. H. and Dudukovic, M. P. (2001). CFD modelling of multiphase flow distribution in catalytic packed bed reactors: scale down issues. *Catalysis Today*, **66**, 209-218.

Krischke, A. M. (2001). Modellierung und experimentelle untersuchung von transportprozessen in durchstr-omten sch-uttungen. *Fortschritt-Berichte VDI*, **3**, 713-720.

Kubie, J. (1988). Influence of containing walls on the distribution of voidage in packed beds of uniform spheres. *Chem. Eng. Sci.*, **43**, 1403-1405.

Kutsovsky, Y. (1996). *Nuclear magnetic resonance imaging of flow and dispersion in bead packs*. PhD Thesis, University of Minnesota.

Lerou, J.J. and Froment, G.F. (1986). *The measurements of void fraction profiles in packed beds*. Chemical Reactor Technology, DeLasa, H.I. (ed.), **110**, 853-861. NATO ASI Series E.

Li, H., Hudgins, R.R. and Chang, K.S. (1991). Equivalent annular model of a multi-tubular shell-side fixed-bed reactor. *Jnl. Am. Inst. of Chem. Eng.*, **37**, 1129-1135.

Logtenberg, S.A., Nijemeisland, M. and Dixon, A.G. (1999). Computational fluid dynamics simulations of fluid flow and heat transfer at the wall-particle contact points in a fixed-bed reactor. *Chem. Eng. Sci.*, **54**, 2433-2439.

Maier, R.S., Kroll, D.M., Bernard, R.S. and Howington, S.E. (2000). Pore-scale simulation of dispersion. *Physics of Fluids*, **12**, 2065-2079.

Martin, H. (1978). Low peclet number particle-to-fluid heat and mass transfer in packed beds. *Chem. Eng. Sci.*, **33**, 913-919.

McGreavy, C., Foumeny, E.A. and Javed, K.H. (1986). Characterisation of transport properties for fixed beds in terms of local bed structure and flow distribution. *Chem. Eng. Sci.*, **41**, 787-797.

Moallemi, H.A. (1989). *Predictive characterisation of packed bed structure*. PhD Thesis, Dept. Chemical Engineering, University of Leeds.

Mueller, G.E. (1992). Radial void fraction distributions in randomly packed fixed beds of uniformly sized spheres in cylindrical containers. *Powder Tech.*, **72**, 269-275.

Nandakumar, K., Shu, Y. and Chuang, K.T. (1999). Predicting geometrical properties of random packed beds from computer simulation. *Jnl. Am. Inst. of Chem. Eng.*, **45**, 2286-2294.

Nolan, G.T. and Kavanagh, P.E. (1995). Random packing of non-spherical particles. *Powder Tech.*, **84**, 199-205.

- Papageorgiou, J.N. and Froment, G.F. (1995). Simulation models accounting for radial voidage profiles in fixed-bed reactors. *Chem. Eng. Sci.*, **50**, 3043-3056.
- Richard, P., Philippe, P., Barbe, F., Bourlès, S., Thibault, X. and Bideau, D. (2003). Analysis by X-ray microtomography of a granular packing undergoing compaction. *Physical Review E*, **68**, 020301.
- Ridgway, K. and Tarbuck, K.J. (1968). Voidage fluctuations in randomly-packed beds of spheres adjacent to a containing wall. *Chem. Eng. Sci.*, **23**, 1147-1155.
- Roshani, S. (1990). *Elucidation of local and global structural properties of packed bed configurations*. PhD Thesis, Dept. of Chemical Engineering, University of Leeds.
- Schneider, F.A., Rippin, W.T. and Newton, E. (1990). Generalised description of fluid flow, void fraction and pressure drop in fixed beds with embedded tubes. *Ind. & Eng. Chem. Res.*, **29**, 968-973.
- Seidler, G.T., Martinez, G., Seeley, L.H., Kim, K.H., Behne, E.A., Zaranek, S., Chapman, B.D. and Heald, S.M. (2000). Granule-by-granule reconstruction of a sandpile from X-ray microtomography data. *Physical Review E*, **62**, 8175-8182.
- Sharma, S., Mantle, M.D., Gladden, L.F. and Winterbottom, J.M. (2001). Determination of bed voidage using water substitution and 3D magnetic resonance imaging, bed density and pressure drop in packed bed reactors. *Chem. Eng. Sci.*, **56**, 587-595.
- Sullivan, S.P., Sani, F.M., Johns, M.L. and Gladden, L.F. (2005). Simulation of packed bed reactors using lattice Boltzmann methods. *Chem. Eng. Sci.*, **60**, 3405-3418.
- Taylor, K., Smith, A., Ross, S. and Smith, M. (2000). CFD modelling of pressure drop and flow distribution in packed bed filters. *Phoenics Jnl. CFD & Apps.*, **13**, 399-413.
- Vatani, A. (1996). *Characterisation of transport processes in packed beds*. PhD Thesis, Dept. Chemical Engineering, University of Leeds.
- Wang, Z., Afacan, A., Nandakumar, K., Chuang, K.T. (2001). Porosity distribution in random packed columns by gamma-ray tomography. *Chem. Eng. & Proc.*, **40**, 209-219.
- Zeiser, T., Lammers, P., Klemm, E., Li, Y.W., Bernsdorf, J. and Brenner, G. (2001). CFD-calculation of flow, dispersion and reaction in a catalyst filled tube by the lattice-Boltzmann method. *Chem. Eng. Sci.*, **56**, 1697-1704.
- Zhang, W., Thompson, K.E., Reed, A.H. and Beenken, L. (2006). Relationship between packing structure and porosity in fixed beds of equilateral cylindrical particles. *Chem. Eng. Sci.*, **61**, 8060-8074.
- Zou, R.P. and Yu, A.B. (1996). Wall effect on the packing of cylindrical particles. *Chem. Eng. Sci.*, **51**, 1177-1180.

List of Figures (in order of reference in text)

Figure 1. Illustration of the pellets and packed beds used in this study. Images are derived from the DigiPac algorithm; a) the cylindrical pellets (HC1-5) packed in conventional beds; b) CA (Centre Annulus); c) TA (Three Annuli); and d) OA (One Annulus) shell-side beds.

Table 1. Numerical data of HC1-5 beds investigated

Figure 2. Comparison of measured (symbol), DigiPac (dashed line) and DigiCGP (solid line) predicted local voidage data for conventional packed beds of hollow cylinders (HC1-5).

Table 2. Experimental dimensions and numerical data of the shell-side beds investigated.

Figure 3. Comparison of measured (symbol), DigiPac (dashed line) and DigiCGP (solid line) predicted local voidage data for beds containing a large Centre Annulus (CA).

Figure 4. Comparison of measured (symbol), DigiPac (dashed line) and DigiCGP (solid line) predicted local voidage data for beds containing Three Annuli (TA).

Figure 5. Comparison of measured (symbol), DigiPac (dashed line) and DigiCGP (solid line) predicted local voidage data for beds containing One Annulus (OA).

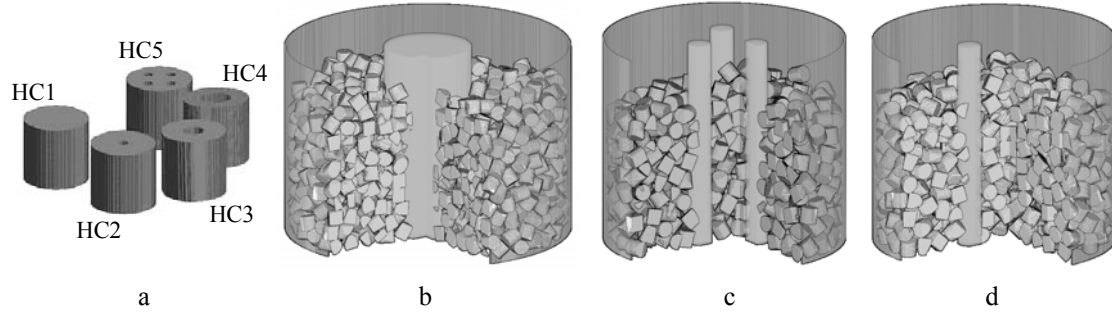


Figure 1

Bed	Number of trial runs			Equivalent pellet diameter, d_{pe} (mm)	d_i/d_{pe}	Bed height, h_i (mm)	Bulk voidage (stdev)				Pellet features
	Experimental	DigiPac	DigiCGP				Measured (average)	DigiPac predicted	DigiCGP predicted	% error (CGP)	
HC1	5	4	4	14.5	7.10	56	0.380 (0.020)	0.416 (0.022)	0.385 (0.019)	1.32	Solid cylinder
HC2	5	4	4	14.4	7.15	52	0.405 (0.025)	0.376 (0.021)	0.389 (0.020)	3.95	2mm central hole
HC3	5	4	4	14.0	7.36	57	0.418 (0.019)	0.421 (0.021)	0.413 (0.017)	1.19	4mm central hole
HC4	5	4	4	13.4	7.69	60	0.479 (0.015)	0.504 (0.014)	0.487 (0.013)	1.67	6mm central hole
HC5	5	4	4	14.0	7.36	55	0.559 (0.024)	0.549 (0.021)	0.564 (0.018)	0.89	4x 2mm holes

Table 1

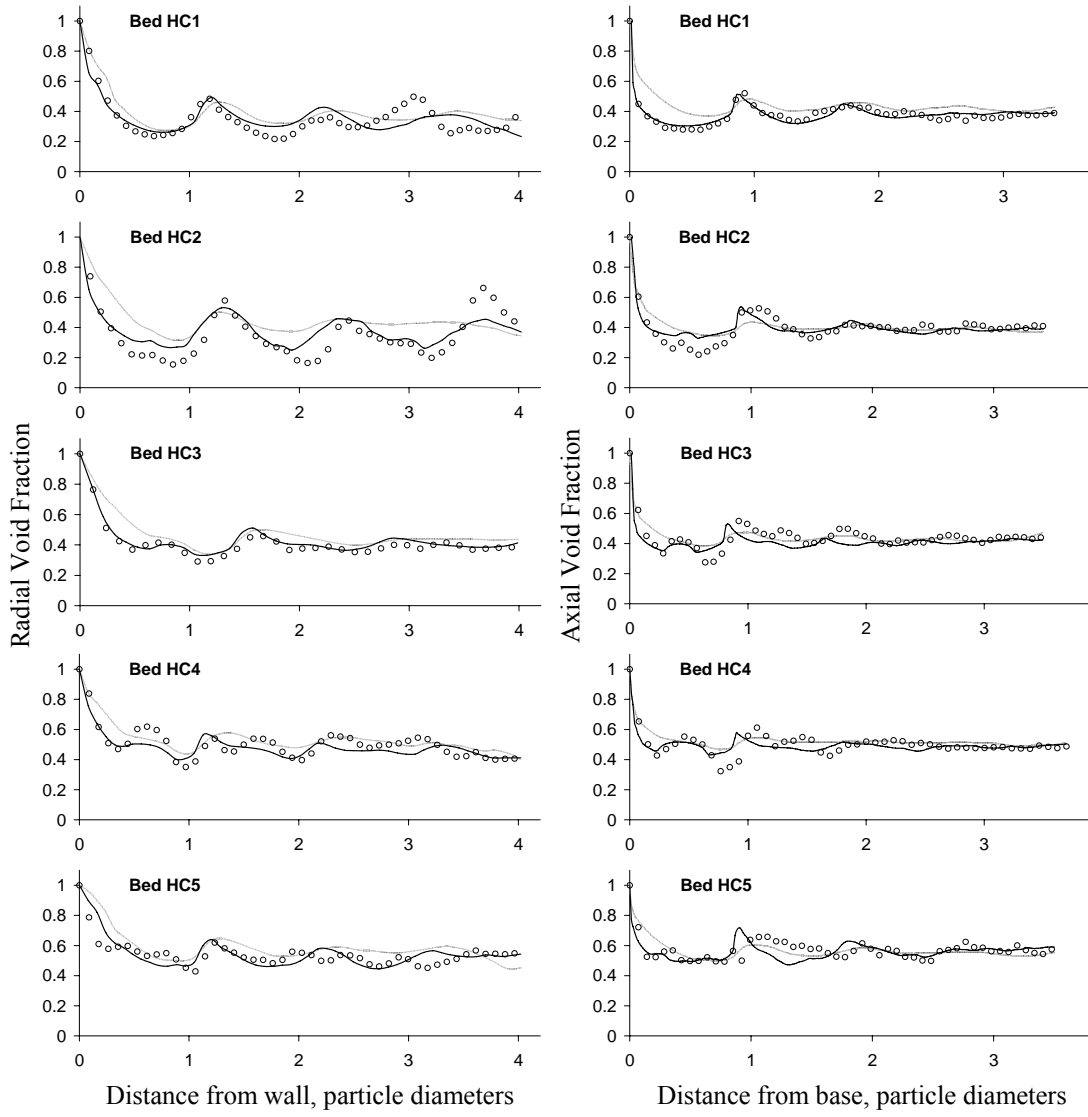


Figure 2

Bed	Number of trial runs			Pellet diameter, d_p / Height, h_p (mm)	d_{pe} (mm)	Bed diameter, d_b / Height, h_b (mm)	d_{le} (mm)	d_{le}/d_{pe}	Bulk voidage (stdev)				Annuli		
	Experimental	DigiPac	DigiCGP						Measured (average)	DigiPac predicted	DigiCGP predicted	% error (CGP)	Number of tubes	Tube diameter (mm)	Dist. between tubes (mm)
CA3	5	4	4	5.3/5.3	5.3	103/61	71.0	13.4	0.395 (0.020)	0.434 (0.022)	0.411 (0.022)	4.05	1	32	-
CA4	5	4	4	5.3/3.6	4.6	103/58	71.0	15.4	0.369 (0.018)	0.422 (0.021)	0.374 (0.021)	1.35	1	32	-
TA1	4	4	4	8.6/8.6	8.6	80/64	59.7	6.9	0.409 (0.016)	0.449 (0.019)	0.422 (0.020)	3.18	3	8	16
TA2	4	4	4	5.3/5.3	5.3	80/59	59.7	11.3	0.348 (0.023)	0.401 (0.022)	0.362 (0.021)	4.02	3	8	16
OA1	4	4	4	8.6/8.6	8.6	80/57	72.0	8.4	0.359 (0.017)	0.386 (0.021)	0.371 (0.019)	3.34	1	8	-
OA2	4	4	4	5.3/5.3	5.3	80/63	72.0	13.6	0.359 (0.021)	0.379 (0.020)	0.370 (0.022)	3.06	1	8	-

Table 2

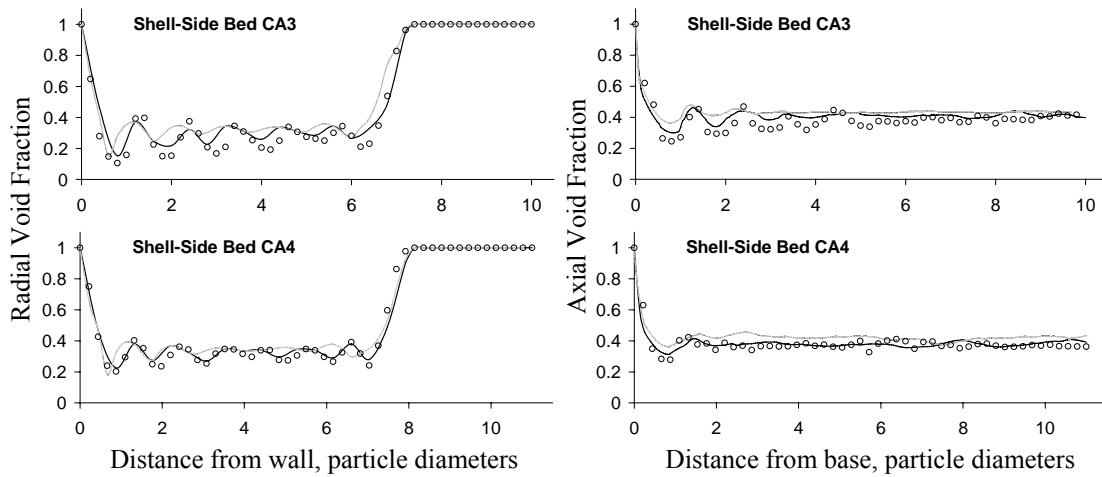


Figure 3

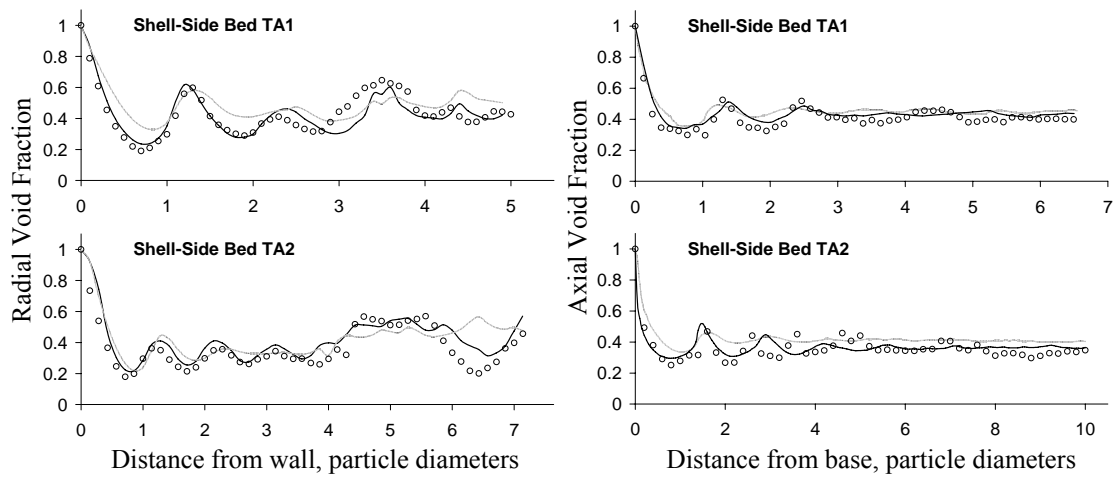


Figure 4

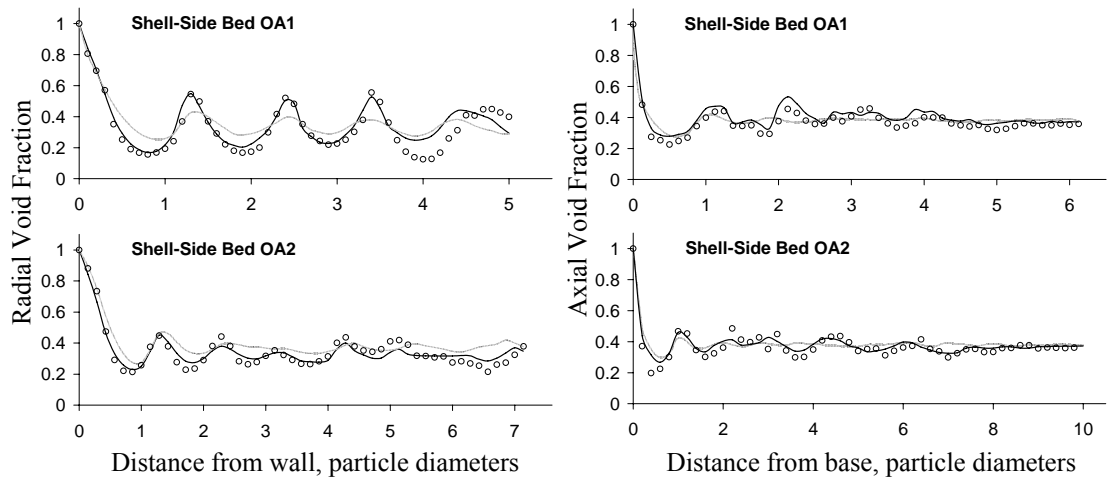
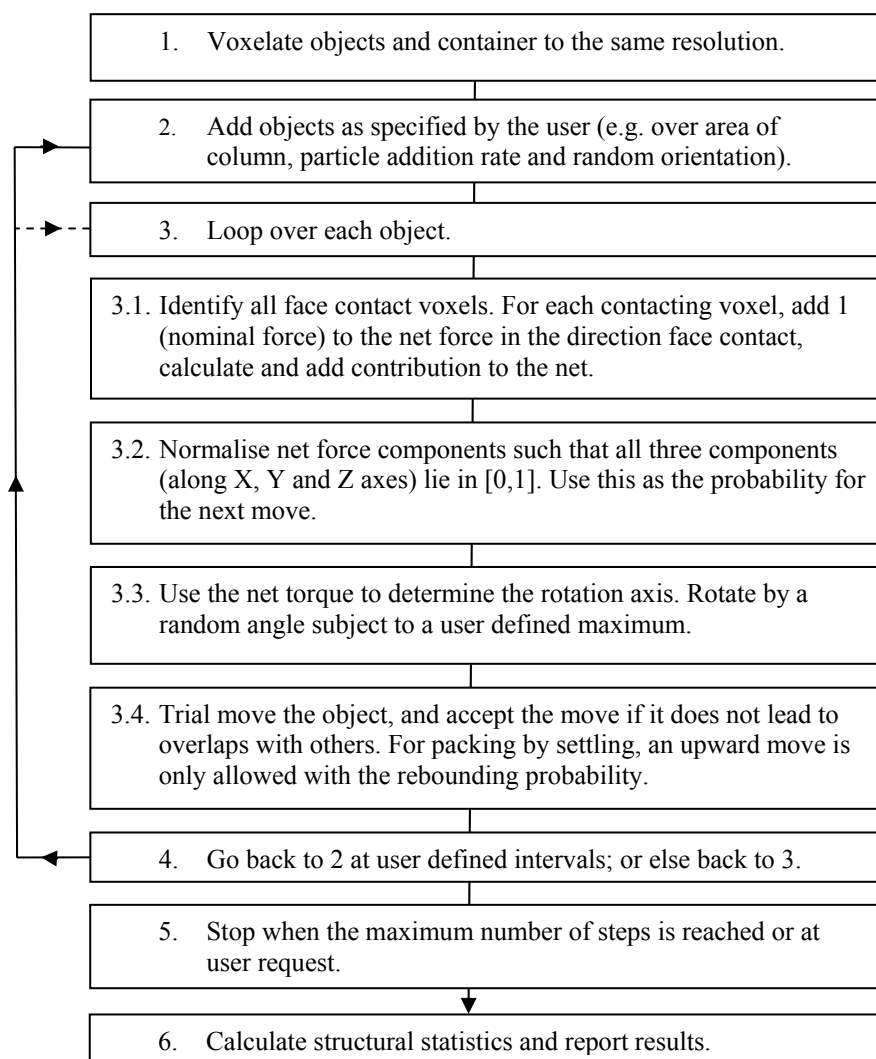


Figure 5

APPENDIX

The original DigiPac model has been described in detail elsewhere (Caulkin et al., 2006). Therefore, for the new DigiCGP model a flow chart is provided, for which, at pixel level, no more than elementary physics concepts are used. The model is a step away from being purely stochastic, by making use of collision points.

DigiCGP Flowchart



An implementation of the above algorithm, which was used by the authors to perform the reported simulations, is available from Structure Vision Ltd. (contact: x.jia@leeds.ac.uk).

For one sample result, we specify the corresponding simulation variables matching the real-life scenario, sufficient for the interested reader to independently reproduce the results with either the model(s) of the authors or other models.

Corresponding data for one sample result: Bed HC4.

Digital simulation resolution: 0.2mm/voxel.

Container dia. (outer): 521 pixels

Container dia. (inner): 515 pixels (103mm)

Container ht: 600 pixels (120mm)

Pellet dia: 64 pixels (12.7mm)

Pellet ht: 64 pixels (12.7mm)

Pellet hole dia: 30 pixels (6mm)

Total number of pellets: 135

Approximate packing ht: 300 pixels (60mm)

Particle addition rate: 3 particles per 100 simulation time steps.

Particle addition method: Hopper mode (Orifice size ratio = 1.0, i.e. particles introduced over whole area of column).

Particles randomly rotated prior to introduction into container

Particles allowed to rotate, based on collisions, once introduced at the top of container

(both rotation methods are 'standard rotation' so particles do not contain holes afterwards)

Particles allowed to free-fall

Rebounding probability: 0.4

Simulation run in DigiCGP mode

Multithreads used

Simulation time: approximately 45 mins

The above conditions were selected to correspond with the following description:

- Particles were deposited from a fixed height (approx. 10x the height of the pellets). To accommodate this, a relatively tall container was used which allowed the pellets to fall freely, colliding with each other and the container wall, inducing pellet rotation, before coming to a rest when they form part of the packing structure.
- Pellets were added at a slow rate, in small batches, allowing them sufficient time to settle by reaching the base of the container or the top of other packed pellets before following ones were introduced.
- After each batch of pellets was introduced, the container was gently vibrated, by means of gentle tapping with a ruler (working from bottom-to-top in an anti-clockwise direction around the column), to encourage the pellets to find a stable position within the packed structure.

Data extraction and analysis

When all the pellets had been introduced and had been given sufficient time to settle, the simulation was stopped and the resulting data was extracted for direct comparison with the experimental results. For the DigiPac/DigiCGP simulations, this was as follows:

- Firstly, the digital structure was saved, excluding the solid cylindrical container in the process.
- For radial voidage measurement, the saved structure was treated as binary data and was analysed by applying 50 equally spaced concentric rings (which corresponded with the analysis of the experimental bed) over the height of the packing (the free space above the packing was excluded, as it would otherwise lead to elevated voidage calculation). The ratio of solid voxels to empty space within each ring was then calculated by the software, and output in spreadsheet format.
- These 50 ratios, which related to packing density in each successive ring (outermost to innermost), were converted to voidage distribution (packing density – 1.0). A

correction factor was then applied to the voidage values to exclude the effect of the cubic bounding box which surrounded the cylindrical container. (cubic packing area = 521×521 pixels; cylindrical packing area = $\pi 257.5^2$; cubic area \div cylindrical area = voidage \div 1.3031 to give true radial values for a cylindrical packed bed).

- Finally, these values were plotted against scaled distance from the container wall in particle diameters. (inner container diameter $(515)/2 = 257.5$; container radius $(257.5)/$ particle diameter $(64) = 4.02$ particle diameters (from outer wall to centre of bed); $4.02/50$ voidage values = cumulative distance (in particle diameters) from container wall for each consecutive ring (0.0804).

Axial voidage measurement

- From the saved digital structure used for radial voidage analysis, axial data (along the Z-axis) was also obtained from the software. The packing density (the fraction of solid to empty voxels) of each bed slice or cross-section, one voxel in height, is automatically calculated by the model software.
- As with radial analysis, the values are converted to voidage, and the same correction factor applied to exclude the effect of the square bounding box.
- The resulting values are then plotted against axial distance from the base of the container in particle diameters.

Bulk voidage measurement

- As stated in the main body of text, bulk voidage is calculated by averaging the axial voidage once end effects have dissipated.

For each of the above measurement criteria, individual bed values were averaged for numerous repackings (see Tables 1 and 2), with the averaged local profiles presented in Figs. 2, 3, 4 and 5, and averaged bulk values shown in Tables 1 and 2.